

**NASA**  
**Technical**  
**Paper**  
**2655**

October 1986

# Jet Model for Slot Film Cooling With Effect of Free-Stream and Coolant Turbulence

Frederick F. Simon

**NASA**

**NASA  
Technical  
Paper  
2655**

1986

**Jet Model for Slot Film  
Cooling With Effect  
of Free-Stream and  
Coolant Turbulence**

Frederick F. Simon

*Lewis Research Center  
Cleveland, Ohio*



National Aeronautics  
and Space Administration

Scientific and Technical  
Information Branch

Reconocimiento  
El autor se siente muy  
agradecido por la ayuda  
DEL SENOR en esta obra

## Summary

An analysis was performed utilizing the model of a wall jet for obtaining equations that will predict slot film-cooling efficiency under conditions of variable turbulence intensity, flow, and temperature. The analysis, in addition to assessing the effects of the above variables, makes a distinction between an initial region and a fully developed region. Such a distinction is important in determining the role that the turbulence intensity of the coolant plays in effecting film-cooling effectiveness in the area of the slot exit. The results of the analysis were used in the correlation of the results of a well-designed film-cooling experiment. The result of the analysis and experiment was equations that predicted film-cooling efficiency within  $\pm 4$  percent average deviation for lateral free-stream turbulence intensities up to 24 percent and blowing rates up to 1.9. These equations should be useful in determining the optimum quantity of cooling air required for protecting the wall of a combustor.

## Introduction

It is important that the quantity of air used to film cool the combustion chamber of a jet engine be sufficient to maintain acceptable wall temperatures without affecting engine performance more than is necessary. Therefore, an important requirement in the design of a high performance gas turbine combustor is a good prediction of film-cooling requirements. Slot film-cooling prediction approaches applicable to a jet combustion chamber must include, in addition to the effects of gas flow, temperature, and slot configuration, the effect that the turbulence level of the combustion gases and the coolant has on the film-cooling efficiency.

Some work has been done to assess the effect of turbulence on the efficiency of slot film cooling. Carlson and Talmor (ref. 1), present correlations for conditions of variable free-stream turbulence and acceleration. In the analysis that was developed to obtain a correlating equation, it is assumed that the amount of hot free-stream gas mixed with the film coolant is proportional to the mass flow in the boundary layer without mass addition. From their correlations of the experimental data they obtain values of a mixing coefficient, which are found to be proportional to the turbulence level. They determined that with higher turbulence intensity of the free-stream the higher the mixing coefficient and the larger the quantity of

hot gas mixed with the film coolant. The correlations of reference 1 are for specific values of the turbulence intensity. No general correlations in terms of the turbulence intensity are presented.

Juhasz and Marek (ref. 2) performed liner film cooling experiments for several slot configurations for conditions in the gas turbine combustor of 1 atm and temperatures up to 1367 K. They found that the film-mass flow rate and the hot-stream turbulence level were more important parameters than slot geometry. The authors of reference 2 attempted to correlate their experimental data by a number of correlating equations found in the literature. The correlation that they recommend is based on a simple one-dimensional mass mixing model where the mixing coefficient is assumed equal to the free-stream turbulence intensity. Using this approach, they were able to correlate this experimental film-cooling efficiency to within  $\pm 20$  percent. The results of reference 2 were for an average value of the combustion chamber turbulence level of 15 percent. The simple mixing model of reference 2 was used in reference 3 in an attempt to correlate the film-cooling experimental data obtained at four levels of free-stream turbulence. In an effort to remove some of the complexities of a combustion chamber, the experiment of reference 3 was run in a rectangular chamber having a controlled turbulence level with a constant free-stream flow and temperature (590 K). They found that film-cooling effectiveness decreased as much as 50 percent for an increase in free-stream axial turbulence intensity from 7 to 35 percent. However, they were not able to obtain a good correlation between turbulence intensity and the calculated turbulent mixing coefficient. The authors of reference 3 utilized a constant value of the mixing coefficient to predict the experimental data within  $\pm 30$  percent.

The work of Sturgess, et al (refs. 4 and 5), makes significant progress in understanding of the role that turbulence plays in slot film cooling and in the presentation of correlating equations. These correlating equations were developed by using functional modifications to an analysis (ref. 6) that assumed boundary layer growth of the wall coolant jet. With this approach, correlating equations are presented for the data of reference 3 (ref. 4). An important feature of these correlations is consideration for the potential core region, which exists in the region of the slot exit. The assumption is made that the film-cooling efficiency is one ( $\eta = 1.0$ ) in the potential core region.

The objective of the present investigation is to extend the

initial film-cooling modeling efforts of Juhasz and Marek (ref. 2) and Marek and Tacina (ref. 3) into a more comprehensive description of the interaction of a coolant jet with a high temperature turbulent free stream. By utilizing a mixing model, which takes into account some of the features of a developing turbulent wall jet, a correlation is developed for a prediction of slot film cooling for conditions of variable flow, variable temperature, and variable turbulence level.

A model of a developing turbulent wall jet caused by the interaction of coolant and free stream is presented in the section Analysis. The model accounts for an initial developing region and a fully developed region. A heat and mass balance is performed for both regions. The entrance region is divided into a fully mixed zone and partially mixed zone to account for the effect of the initial turbulence level of the coolant jet. A jet model is utilized which grows in proportion to the transverse velocity fluctuation and the blowing ratio  $M$ . An analysis of Abramovich (ref. 7) is utilized to determine the transition point between the initial and fully developed regions. Constants in the developed equations are determined from the controlled experimental data of reference 3. Finally, a test of the developed correlations is made by comparing predictions with the experimental data of reference 3.

## Symbols

$a_o$	constant, equation (14)
$b$	wall-jet thickness
$C_M$	turbulent mixing coefficient, equation (10)
$C_o$	constant, equation (7)
$F(R)$	jet interface position function, equation (25)
$f(x)$	fraction of coolant mass flow rate, equation (A31)
$g(x)$	fraction of diffused mass flow rate, equation (A32)
$I_v$	transverse turbulence intensity, based on free-stream velocity, equation (18)
$I_v^*$	transverse turbulence intensity, equation (A50)
$M$	blowing parameter, $\rho_s \bar{U}_s / \rho_\infty \bar{U}_\infty$
$m$	mass flow rate per unit span
$N$	constant, equation (20)
$R$	velocity ratio
$S$	injection slot height
$T$	absolute temperature
$U^*$	jet characteristic velocity
$U$	gas velocity
$v'$	fluctuating velocity normal to surface being cooled (rms value)
$x$	distance downstream of slot exit
$y_1$	wall-jet/coolant interface position, (see fig. 1)
$y_2$	wall-jet/free-stream interface position, (see fig. 1)

$\beta$	initial region factor, equation (4)
$\eta$	film-cooling effectiveness
$\eta'$	film-cooling effectiveness of fully mixed initial region, equation (A42)
$\theta$	dimensionless temperature ratio, equation (5)
$\rho$	gas density
$\phi$	dimensionless wall-jet thickness, $b/S$
$\psi$	dimensionless temperature ratio, equation (6)
$\omega$	dimensionless flow-temperature grouping, equation 20

## Subscripts

$aw$	adiabatic wall
$exp$	experimental
$s$	coolant
$T$	total
0	position of coolant injection, (see fig. 1)
1	point of transition between initial and fully developed region, (see fig. 1)
I	zone I of jet, (see fig. 1)
II	zone II of jet, (see fig. 1)
$\infty$	hot gas

## Superscripts

—	average quantity
---	------------------

## Analysis

Figure 1 depicts the situation of a secondary fluid (coolant) at a low temperature ( $T_s$ ) being injected at the wall of a chamber with a rectangular cross section through which flows a high temperature gas. The model of figure 1 simplifies the situation occurring at the liner of a jet engine combustor. The effect of the hot and cold streams meeting at the slot exit is the creation of a semicontained turbulent jet whose thickness  $b$  grows with distance  $x$ , and whose properties are determined by the amount of free-stream fluid entrained  $m_\infty$ . The turbulent jet has an initial developing region, sometimes called the "potential core" region. This region has very efficient cooling as indicated by the use of temperature sensitive paints on a combustor liner (ref. 8). The length of this region  $x_1$  is assumed for the present analysis to be the distance required for the inner edge of the growing/mixing zone I (fig. 1) to reach the wall. Since zone II of the initial region consists mostly of coolant fluid, some researchers have assumed that the wall temperature in this region is at or near the inlet coolant temperature  $T_s$ . Realistically, some fluid ( $m_1$ ) from the turbulent mixing zone I will be entrained into zone II and raise the temperature in this zone above the value of the inlet coolant temperature  $T_s$ . Since the analysis is for an adiabatic wall, the

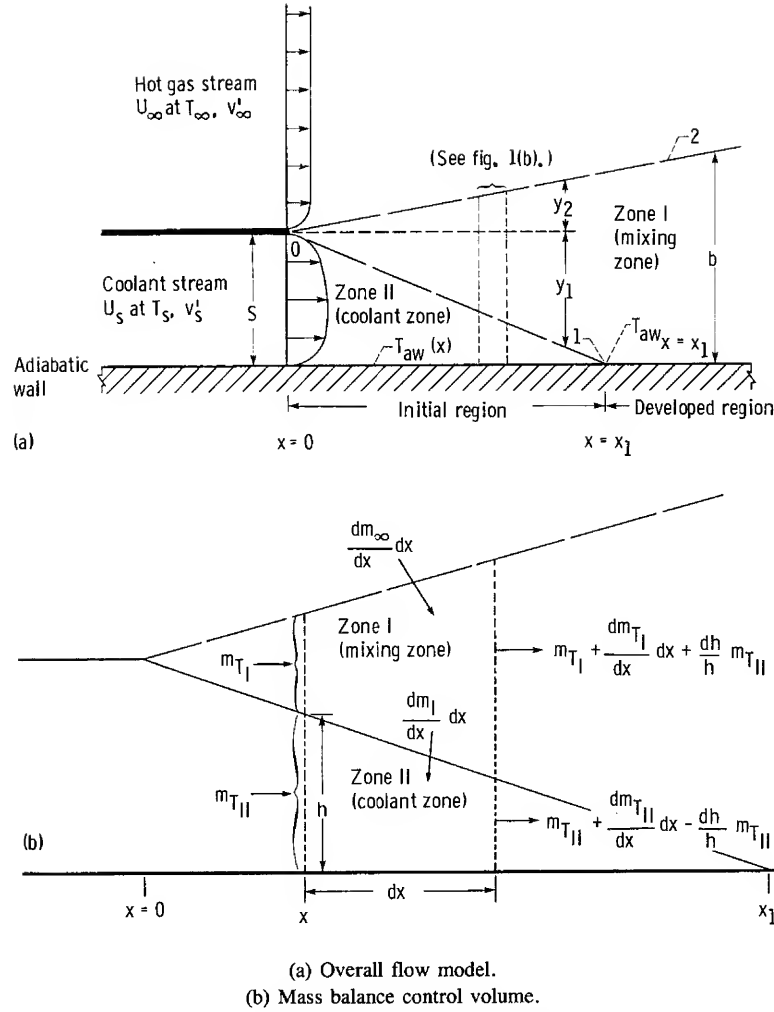


Figure 1.—Slot film-cooling flow model.

wall surface temperature  $T_{aw}$  is assumed equal to the mean fluid temperature  $\bar{T}$ . In the initial region, the adiabatic wall temperature is assumed equal to the mean fluid temperature in zone II

$$T_{aw} = \bar{T}_{II} \quad (x < x_1) \quad (1)$$

In the developed region the adiabatic wall temperature is assumed equal to the mixing temperature of the turbulent jet

$$T_{aw} = \bar{T}_I \quad (x \geq x_1) \quad (2)$$

The following additional assumptions are made:

- (1) The axial pressure drop of the wall jet is negligible
- (2) The change in the specific heat with temperature is small
- (3) The composition of the mainstream and coolant is the same
- (4) The hot gas temperature  $T_\infty$  is constant
- (5) The hot stream thermal radiation is negligible
- (6) Interfaces (0-1 and 0-2, fig. 1) of the developing wall jet are linear

With the above assumptions, a differential mass flow rate and energy balance are made of zones I and II (fig. 1b), in order to relate the film-cooling efficiency to the growth of the wall jet. Details of the analysis are given in appendix A. The equations derived for the initial region and the fully developed region are as follows:

#### Initial Region $x < x_1$

In the initial region, the film-cooling effectiveness is

$$\eta = \frac{1 + \beta}{1 + \left(\frac{x}{MS}\right) \left(\frac{(\phi - 1)S}{x}\right)} \quad (3)$$

Here  $\beta$  may be expressed in terms of dimensionless temperature ratios

$$\beta_{\exp} = \left[ \frac{x}{x_1} \left( \frac{\phi_1 - 1}{M} + 1.0 \right) - \left( 1 - \frac{x}{x_1} \right) \theta \right] \psi \quad (4)$$

$$\theta = \frac{T_{aw} - T_s}{T_{aw_{x=x_1}} - T_{aw}} \quad (5)$$

$$\psi = \frac{T_{aw_{x=x_1}} - T_{aw}}{T_\infty - T_s} \quad (6)$$

or in terms of a dimensionless temperature ratio and turbulent diffusion from zone I to zone II

$$\beta = \left[ \frac{x}{x_1} \left( \frac{\phi_1 - 1}{M} + 1.0 \right) - \left( \frac{x_1 - x}{x_1} \right) C_o I_{v,s}^* \frac{T_s}{T_{aw_{x=x_1}}} \ln \left( \frac{1}{1 - \frac{x}{x_1}} \right) \right] \psi \quad (7)$$

Equation 7 may be used, as shown later, in conjunction with equation 3 for predictive purposes. The constant  $C_o$  can be determined by using experimental data.

#### Developed Region $x \geq x_1$

In the developed region the value of  $\beta$  is zero and equation 3 reduces to

$$\eta = \frac{1}{1 + \left( \frac{x}{MS} \right) \left( \frac{(\phi - 1)S}{x} \right)} \quad (8)$$

Equation (8) can be expressed in terms of a turbulent mixing coefficient  $C_M$  (refs. 2 and 3) as follows:

$$\eta = \frac{1}{1 + \frac{x}{MS} C_M} \quad (9)$$

where the turbulent mixing coefficient in the present analysis is a function of the jet boundary layer growth rate

$$C_M = \frac{(\phi - 1)S}{x} \quad (10)$$

The efficiency equations (3) and (8) for the initial and developed regions may be expressed in a general equation

$$\eta = \frac{1}{1 + \left( \frac{x}{MS} \right) C'_M} \quad (11)$$

where

$$C'_M = \frac{C_M - \frac{\beta}{\left( \frac{x}{MS} \right)}}{1 + \beta} \quad (12)$$

The equation  $\beta$  (eq. (7)) is expressed in terms of the turbulent mixing coefficient  $C_M$  (eq. (10))

$$\beta = \left[ C_M \left( \frac{x}{MS} \right) + \frac{x}{x_1} - \left( \frac{x_1 - x}{x} \right) C_o I_{v,s}^* \frac{T_s}{T_{aw_{x=x_1}}} \ln \left( \frac{1}{1 - \frac{x}{x_1}} \right) \right] \psi \quad (13)$$

with the following conditions:

$$x \geq x_1 \quad \begin{cases} \beta = 0 \\ C'_M = C_M \end{cases}$$

#### Turbulent Mixing Coefficient $C_M$

Abramovich (ref. 7, pg. 37) assumes the growth of the jet boundary layer  $b$  to be proportional to the perturbation component of the transverse velocity. This may be expressed as

$$\frac{db}{dx} = \frac{a_o v'}{U^*} \quad (14)$$

While both the transverse velocity fluctuation  $v'$  and the characteristic velocity  $U^*$  are both likely to vary with  $x$ , the experimental evidence for turbulent jets suggest a near linear jet growth rate. Therefore, it is assumed that edge 0-2 (fig. 1) is linear in  $x$ . Equation (14) may then be expressed as

$$\frac{db}{dx} = \left( \frac{db}{dx} \right)_{x=0} = \frac{a_o v'_o}{U_o^*} \quad (15)$$

Following the approach of reference 9 for the characteristic velocity  $U^*$  of the mixing of two streams with different velocities and densities, the characteristic velocity at  $x = 0$  for the model of figure 1 is

$$U_o^* = \frac{\rho_\infty \bar{U}_\infty + \rho_s \bar{U}_s}{\rho_\infty + \rho_s} \quad (16)$$

which can be written as

$$U_o^* = \frac{\bar{U}_\infty [1 + M]}{1 + \frac{T_\infty}{T_s}} \quad (17)$$

Defining a transverse turbulent intensity as follows:

$$I_v = \frac{v_o'}{\bar{U}_\infty} \quad (18)$$

and substituting equations (17) and (18) into equation (15) results in

$$\frac{db}{dx} = \frac{a_o I_v \left(1 + \frac{T_\infty}{T_s}\right)}{(1 + M)} \quad (19)$$

A more general form of equation (19) is

$$\frac{d\phi}{dx} = \frac{a_o (I_v \omega)^N}{S} \quad (20)$$

where

$$\omega = (1 + T_\infty/T_s)/(1 + M)$$

Integration of equation (20) results in an expression for the turbulent mixing coefficient

$$C_M = \frac{(\phi - 1)S}{x} = a_o (I_v \omega)^N \quad (21)$$

The work of Juhasz and Marek (ref. 2) assumed the mixing coefficient to be proportional to the transverse turbulent intensity, but they did not consider the effect of temperature and blowing rate indicated in equation (21).

Ko and Liu (ref. 10) state that the turbulent intensity distribution for the main stream and the wall jet have a great influence on the film-cooling efficiency. In their calculation of the mixing coefficient, according to that proposed in

reference 3, they considered the turbulence of the free stream and of the wall jet. Therefore, the effective value of lateral turbulent fluctuation  $v_o'$ , to be used in equation (18) is some function of the fluctuation of the free stream  $v_{\infty,o}'$  and of the wall jet  $v_{s,o}'$ . Based on the recommendation of reference 10 the following relationship is utilized:

$$v_o' = \bar{v}_{\infty,o}' + 0.4(|\bar{v}_{s,o}' - \bar{v}_{\infty,o}'|) \quad (22)$$

or in terms of the defined intensity (eq. (18))

$$I_v = I_{v,\infty} + 0.4(|I_{v,s} - I_{v,\infty}|) \quad (23)$$

with the condition that the value of  $I_v$  is not greater than both  $I_{v,\infty}$  and  $I_{v,s}$ .

Equation (23) suggests that at high free-stream turbulence the turbulence of the free stream has the dominant effect on the film cooling efficiency than does the turbulence of the wall jet.

#### Initial Region Length $x_1$

To determine the length of the initial region  $x_1$  it is necessary to know the position of the interface 0-1 with respect to the lip of the coolant slot  $y_1$  (fig. 1). Abramovich (ref. 7, pg. 163), using a momentum and mass balance for the two streams, determined analytically the relationship between interface positions 0-2 and 0-1. His result can be expressed as follows:

$$\frac{y_1}{y_2} = \frac{1}{\frac{1}{\frac{\bar{\rho}_1}{\rho_s} (0.416 + 0.134 R)} - 1.0} \quad (24)$$

$$R = \frac{\bar{U}_\infty}{\bar{U}_s}$$

$$\frac{\bar{\rho}_1}{\rho_s} = \frac{T_s}{\bar{T}_1}$$

using equation (A25) equation (24) is expressed as

$$\frac{y_1}{y_2} = \frac{1}{\frac{1}{\frac{T_s}{T_{aw,x=x_1}} (0.416 + 0.134 R)} - 1.0} = F(R) \quad (25)$$

From the geometry of figure 1 the following is obtained:

$$y_2 = S(\phi - 1) \quad (26)$$

$$x_1 = \frac{S}{y_1} x \quad (27)$$

Substituting equations (26) and (27) into equation (25) and making use of equation (10) results in the following expression for the entrance length:

$$x_1 = \frac{1}{\left(\frac{C_M}{S}\right) F(R)} \quad (28)$$

Use of equation (28) requires an initial estimate of  $x_1$  so that a value of the wall temperature at  $x = x_1$  ( $T_{aw, x=x_1}$ ) may be determined. This permits use of equation (28) to calculate  $x_1$  and an iteration routine for the exact value of  $x_1$  (appendix B).

## Experimental Data

To enable the equations developed in the section Analysis to be suitable for predicting film-cooling efficiencies it is required that the constants  $a_o$ ,  $N$ , and  $C_o$  in equations (21) and (13) be determined. This was accomplished by the use of the experimental film-cooling data of reference 3. Reference 3 reported film-cooling data at four levels of free-stream turbulence for a constant free-stream velocity (62 m/sec), constant free-stream temperature (590 K), constant pressure (1 atm), ambient inlet temperature of coolant and four film-cooling flow rates. The experiment was designed so that a more controlled and simplified version of a jet engine combustor would be possible without the complications of the large temperature and velocity gradients which exist in an actual combustor. In the experiment of reference 3 preheated gases were passed through turbulence generators and then through a 10.5- by 37-cm rectangular duct, which contained provision for slot film cooling on one surface. This surface was insulated to permit an adiabatic wall condition. Wall surface temperatures were taken of the surface being film cooled at nine positions downstream of the exit slot position. The temperature measurement at the end (9th) location was not utilized in this paper because of a wall conduction error. Axial and transverse turbulence of the free stream and coolant were measured with a hot wire.

## Results

### Constants $a_o$ and $N$

As part of the procedure to determine the constants  $a_o$  and  $N$  in equation (21) values of the dimensionless jet boundary

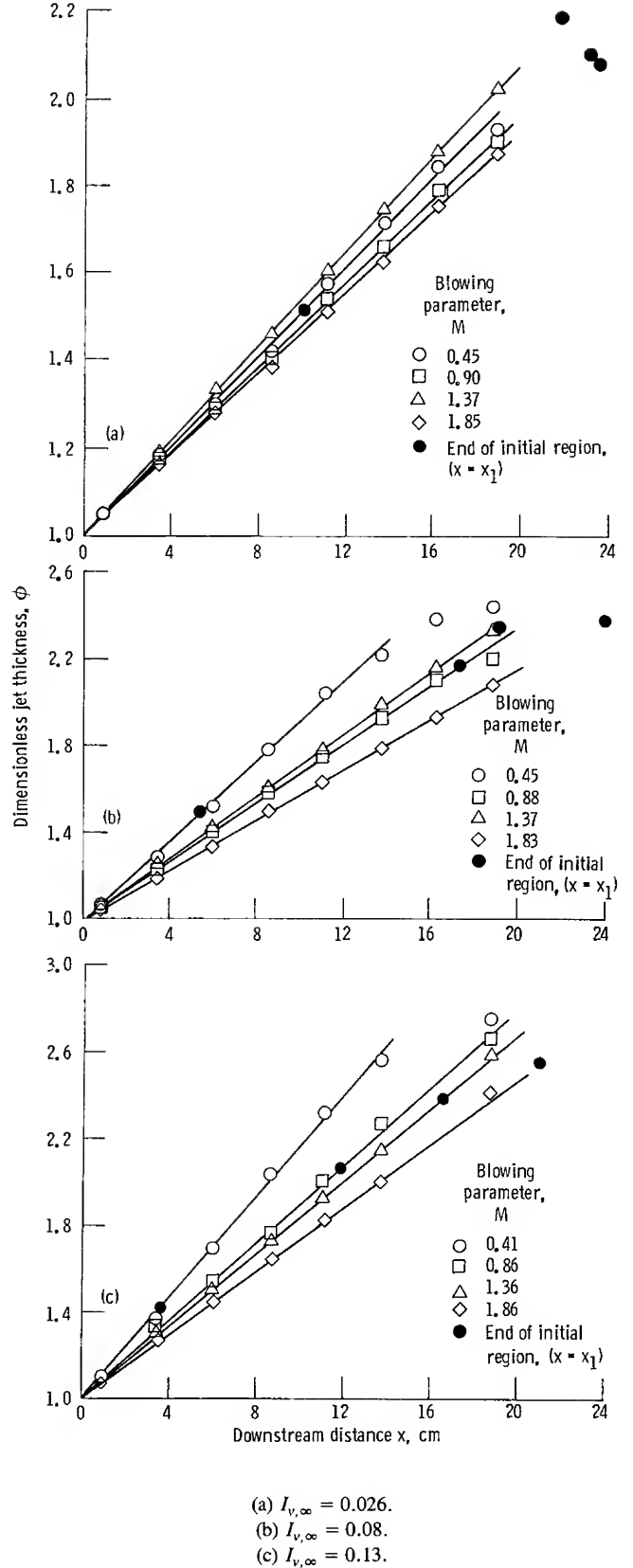
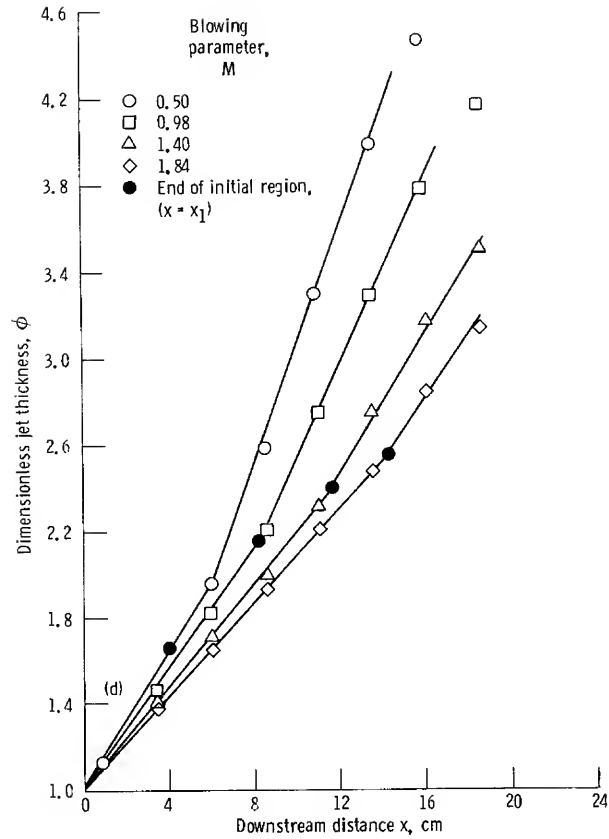


Figure 2.—Calculated dimensionless wall-jet thickness as a function of distance from the slot exit for a given free-stream turbulence.



(d)  $I_{v,\infty} = 0.244$ .

Figure 2.—Concluded.

thickness ( $\phi$ ) were determined by using equations (3), (8), and (28) and the experimental values of reference 3. Calculated values of the initial length  $x_1$  and the dimensionless jet boundary layer are given in table I and figure 2.

Figure 2 indicates that for the lowest three turbulence levels there is a linear relationship between the jet boundary layer and the distance  $x$ . Such linearity is consistent with other measurements and analyses of a wall jet. If the initial region effect had been neglected and the equation for the fully developed region had only been used (eq. (8)) then a nonlinear variation in the jet boundary layer would have resulted. In terms of the film-cooling efficiency (eq. (3)), the effect of  $\beta$  (eq. (4)) in the initial region is about 10 percent in the experiments of reference 3. For the highest value of free-stream turbulence ( $I_{v,\infty} = 0.244$ , fig. 2(d)) there is a noted change in slope at each value of the blowing factor  $M$  for values of the distance  $x$  greater than the distance of the initial region  $x_1$ . Figure 2(d) shows that this slope change occurs at the beginning of the fully developed region  $x = x_1$ . The slopes of the curves of figure 2 for all values of the free-stream turbulence varies with the blowing factor. Slopes of the curves of figure 2 and values of  $\omega$  (eq. (20)) are given in table II. A slight adjustment was made in the determination of the slope

for  $I_{v,\infty} = 0.244$  and  $M = 0.5$  (fig. 2(d)) by having the line for the fully developed region pass through the transition point ( $x = x_1$ ). This introduced a very slight error and made it possible to present a single equation for the mixing coefficient  $CM$  of the fully developed region at the highest turbulent level ( $I_{v,\infty} = 0.244$ ).

Values of the effective lateral turbulence  $I_v$  are also shown in table II. These were calculated by utilizing equation (23), the experimental values of the free-stream lateral turbulence intensity  $I_{v,\infty}$  and the value of the jet lateral turbulence intensity  $I_{v,s}$ . Average values of the jet turbulence were obtained (personal communication with C.J. Marek, Oct., 1985) of the experiment being utilized in this report at the highest blowing rate ( $M = 1.85$ ). Values of the jet turbulence at other blowing rates were calculated by assuming a constant turbulence intensity at the jet exit.

Equation (20) suggests that a log-log plot of the slopes of figure 2 ( $d\phi/dx$  of table II) compared to the product of the effective turbulence  $I_v$  and  $\omega$  should result in a linear curve of slope  $N$ . This is demonstrated in figure 3. The slope of figure 3 is 0.65 or  $N = 0.65$ . With this value for  $N$ , a plot is made as shown in figure 4 to determine the values of  $a_o$ .

As a result of the above procedure for determining  $a_o$  and  $N$ , the following expressions for the mixing coefficients were obtained:

For

$$\begin{aligned} I_{v,\infty} &= 0.026 \\ &= 0.08 \\ &= 0.13 \end{aligned}$$

TABLE I.—LENGTH OF THE INITIAL REGION  $x_1$

$I_{v,\infty}$	$M$	$x_1, \text{cm}$		
		Calculated	Calculated	Experimental
0.026	0.45	9.79	34.44	39
	.90	23.80	41.89	>33
	1.37	26.53	30.79	>22
	1.85	35.08	30.09	>16
0.08	0.45	5.45	19.30	36
	.88	16.35	29.52	30
	1.37	19.97	23.14	>22
	1.83	28.08	24.34	>16
0.13	0.41	3.50	13.52	37
	.86	11.77	21.68	25
	1.36	16.52	19.34	20
	1.86	20.62	17.59	>16
0.244	0.50	4.00	12.81	20
	.98	8.34	13.44	13
	1.40	11.84	13.45	8
	1.84	14.29	12.36	10

TABLE II.—CALCULATED WALL-JET GROWTH RATES

$M$	$I_{v,s}$	$I_v$	$d\phi/dx$	$\frac{\omega, (1 + T_\infty/T_s)}{(1 + M)}$
$I_{v,\infty} = 0.026$				
0.45	0.033	0.029	0.0517	1.902
.90	.062	.040	.0485	1.517
1.37	.090	.052	.0546	1.239
1.85	.119	.063	.0468	1.050
$I_{v,\infty} = 0.08$				
0.45	0.033	0.08	0.0918	1.879
.88	.062	.08	.067	1.516
1.37	.090	.084	.071	1.224
1.83	.119	.096	.057	1.054
$I_{v,\infty} = 0.13$				
0.41	0.033	0.13	0.117	1.875
.86	.062		.089	1.486
1.36	.090		.083	1.208
1.86	.119		.073	1.013
$I_{v,\infty} = 0.244$ (Initial region)				
0.50	0.033	0.244	0.162	1.776
.98	.068		.139	1.400
1.40	.090		.118	1.194
1.84	.119		.108	1.028
$I_{v,\infty} = 0.244$ (Fully developed region)				
0.50	0.033	0.244	0.233	1.776
.98	.068		.217	1.400
1.40	.090		.160	1.194
1.84	.119		.143	1.028

the equation of the turbulent mixing coefficient for the initial and fully developed regions is

$$C_M = 0.177 (I_v \omega)^{0.65} \quad (29)$$

and for  $I_{v,\infty} = 0.244$  the mixing coefficient for the initial region is given by equation (29), while for the fully developed region the value of the coefficient is given by

$$C_M = \left[ 0.245 \left( 1 - \frac{x_1}{x} \right) + 0.177 \frac{x_1}{x} \right] (I_v \omega)^{0.65} \quad (30)$$

#### Constant $C_o$

The constant  $C_o$  in equation (13) may be determined by equating the value of  $\beta$ , in equation (13), to the experimental value of  $\beta$  (eq. (4)), by solving for  $C_o$ , and by using the experimental data of reference 3. Estimates of the conduction

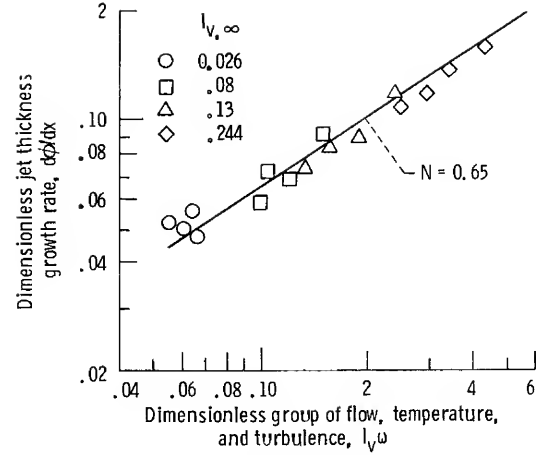


Figure 3.—Determination of the constant  $N$  (eq. (20)).

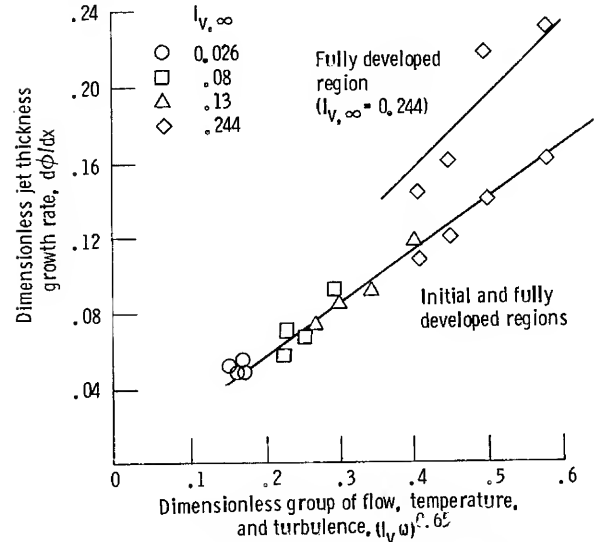


Figure 4.—Determination of the constant  $a_o$  (eq. (20)).

error in the region of the slot entrance for the data of reference 3 ranged from less than 1 percent to 4 percent error in the wall temperature. The conduction error effect on the calculation of  $C_o$  was negligible. To meet the requirement of a true constant for  $C_o$  it was necessary to simplify equation (13) as follows:

$$\beta = \left[ C_M \left( \frac{x}{MS} \right) + \frac{x}{x_1} - C_o I_{v,s}^* \left( \frac{T_s}{T_{aw,x=x_1}} \right) \ln \left( \frac{1}{1 - \frac{x}{x_1}} \right) \right] \psi \quad (31)$$

The average value of the constant  $C_o$  determined was  $C_o = 13.7$ . The value of the average intensity  $I_{v,s}^*$  of the coolant used in calculating  $C_o$  (as determined from the personal communication with C.J. Marek, Oct., 1985) was 0.089.

### Prediction of Film-Cooling Effectiveness

The following equations are the result of the above analytical and experimental considerations:

$$\eta = \frac{1}{1 + \left(\frac{x}{MS}\right) C'_M} \quad (32)$$

$$C'_M = \frac{C_M - \frac{\beta}{\left(\frac{x}{MS}\right)}}{1 + \beta} \quad (33)$$

**Initial Region**  $x < x_1$ .—The values of  $\beta$  and  $C_M$  for prediction of film-cooling efficiency for the initial region are given by

$$\beta = \left[ C_M \left( \frac{x}{MS} \right) + \frac{x}{x_1} - 13.7 I_{v,s}^* \left( \frac{T_s}{T_{aw,x=x_1}} \right) \ln \left( \frac{1}{1 - \frac{x}{x_1}} \right) \right] \psi \quad (34)$$

$$\psi = (T_{aw,x=x_1} - T_{aw}) / (T_\infty - T_s) \quad (35)$$

$$x_1 = \frac{1}{\left(\frac{C_M}{S}\right) F(R)} \quad (36)$$

$$F(R) = \frac{1.0}{\frac{1.0}{\left(\frac{T_s}{T_{aw,x=x_1}}\right) (0.416 + 0.134 R)} - 1.0} \quad (37)$$

$$R = \frac{\bar{U}_\infty}{\bar{U}_s}$$

**Fully Developed Region**  $x \geq x_1$ .—The value of  $\beta$  to predict the film-cooling efficiency for the fully developed region is

$$\beta = 0 \quad (38)$$

for  $I_{v,\infty} = 0.026 - 0.13$

$$C_M = 0.177 (I_{v,\infty})^{0.65} \quad (39)$$

and for  $I_{v,\infty} = 0.244$

$$C_M = \left[ 0.245 \left( 1 - \frac{x_1}{x} \right) + 0.177 \frac{x_1}{x} \right] (I_{v,\infty})^{0.65} \quad (40)$$

$$\omega = \frac{\left( 1 + \frac{T_\infty}{T_s} \right)}{(1 + M)} \quad (41)$$

$$I_v = I_{v,\infty} + 0.4 (|I_{v,\infty} - I_{v,s}|) \quad (42)$$

with the condition that  $I_v$  is not greater than both  $I_{v,\infty}$  and  $I_{v,s}$ .

With the above equations and the calculation scheme of appendix B, predictions were made of the film-cooling efficiencies for the flow, temperatures, and turbulence conditions reported in reference 3. The resulting predictions for film-cooling efficiencies and their comparisons with the experimental data of reference 3 are shown in figure 5. Comparisons between prediction and experiment are generally quite good with an average deviation between prediction and experiment being  $\pm 4$  percent.

### Discussion

The important role played by the transverse velocity fluctuation, as postulated in reference 3, in determining the turbulent mixing coefficient  $C_M$ , is given further confirmation in the present work. In addition, the use of a jet model has brought out two other variables of importance; namely, the blowing ratio  $M$  and a temperature ratio  $T_\infty/T_s$ . The forms of the turbulent mixing coefficient presented herein do a good

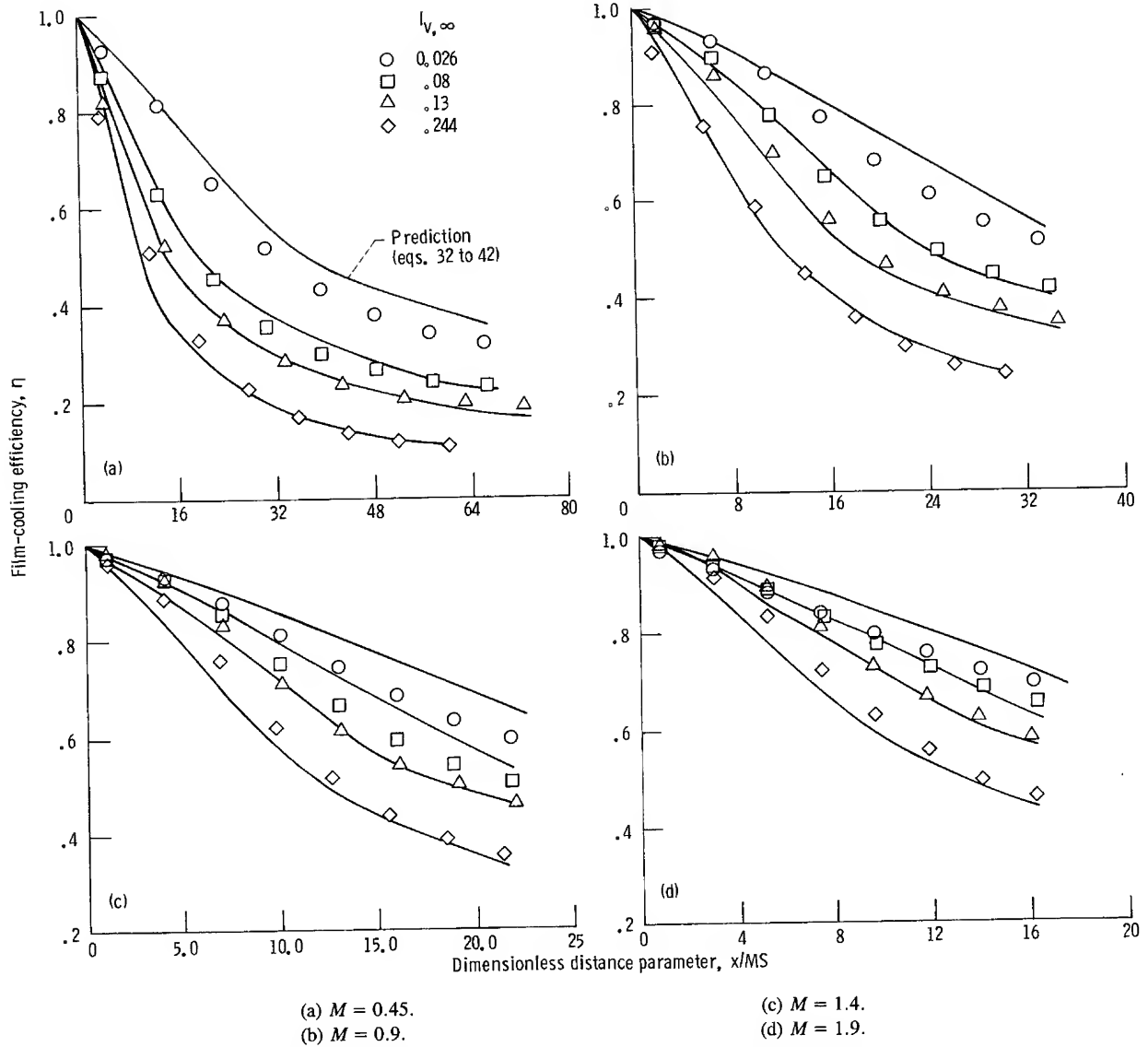


Figure 5.—Comparison of predicted film-cooling efficiencies with experiment.

job of correlating the experimental mixing coefficients of reference 3. The developed equations and experimental data (fig. 5) bring out the important roles played by both the free-stream turbulence and the blowing ratio. At low blowing ratio  $M = 0.45$  (fig. 5(a)), the effect of turbulence is more pronounced than at the higher blowing ratios (e.g.  $M = 1.9$ , fig. 5(d)). These competing effects need to be considered in any design exercises for the optimum cooling of a surface.

The calculated length of the initial region  $x_1$  was found to increase with increases in blowing ratio and decrease with increases in free-stream turbulence (table I). These lengths are significant in their magnitude and for some conditions are larger than the length of the experimental measurements (ref. 3) utilized in the present work. An estimate of the experimental value of  $x_1$  may be made by using equations (32), (33), and (40) as a guide for presenting the experimental

data. For the turbulence range of  $I_{v,\infty} = 0.026$  to 0.13, a plot of  $1/\eta - 1$  compared with  $x/MS$  should result in the fully developed region having a linear correlation that intersects the origin. This is shown in figure 6(a) for the data of reference 3. The point at which the fully developed region begins should establish the length of the initial region. For the highest turbulence level ( $I_{v,\infty} = 0.244$ ), equation (40) suggests that the linear part of the correlation should intersect the  $x/MS$  axis. This is demonstrated in figure 6(b). The experimental values of  $x_1/MS$  are given in table I. Except for the lowest blowing factor, there is general agreement between the calculated and experimental values of the initial region distance parameter ( $x_1/MS$ ).

The correlating equations developed in this paper make a distinction between an initial and a developed region. Such a distinction, in addition to providing a more accurate jet

model, gives some insight into the effect of the initial turbulence level of the coolant on film-cooling efficiency. Results of the calculations for two coolant turbulence levels ( $I_{v,s}^*$ ) at high and low free-stream turbulence are shown in figure 7. In figure 7, the effect of coolant turbulence on film-cooling efficiency is evident in the initial region. The initial region for the higher free-stream turbulence (0.13) ends at the intersection of the two curves for  $I_{v,\infty} = 0.13$ . In the case of the lower free-stream turbulence, transition to the fully-developed region occurs at a value of  $x/MS$  greater than shown in figure 7. Figure 7 is a confirmation of the well known effect of slot turbulence on the film-cooling efficiency and suggests that the effect is more dominant (overall) for conditions of low free-stream turbulence as indicated in references 2 and 6.

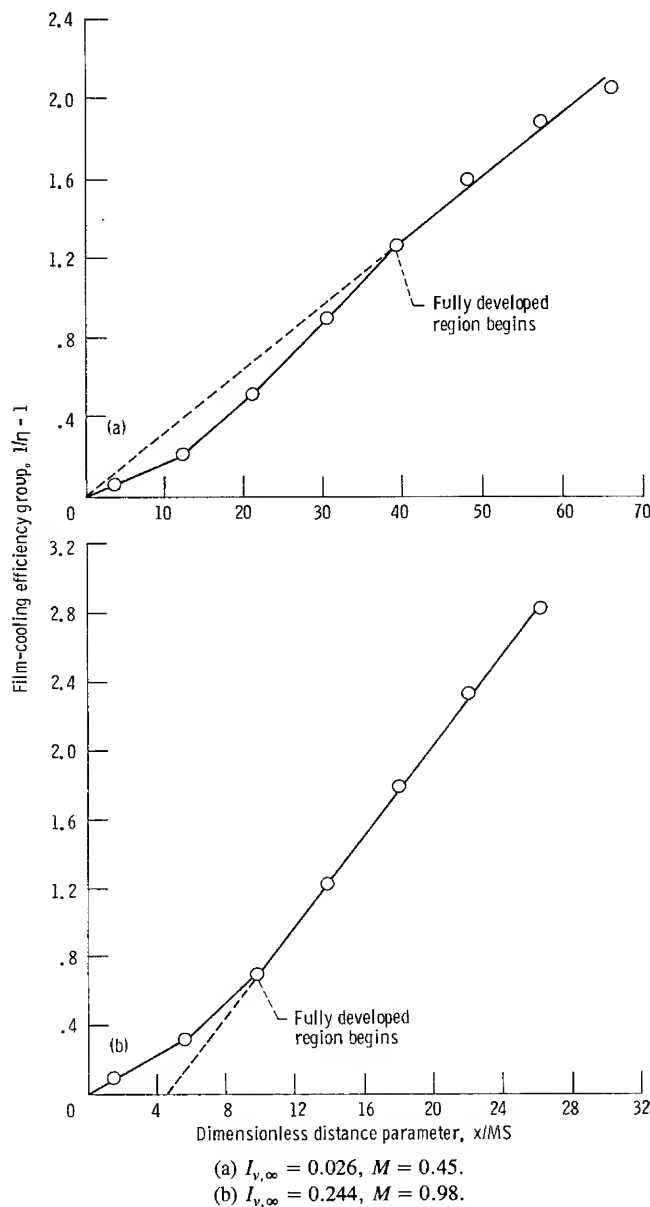


Figure 6.—Experimental determination of the initial region distance parameter  $x_1/MS$ .

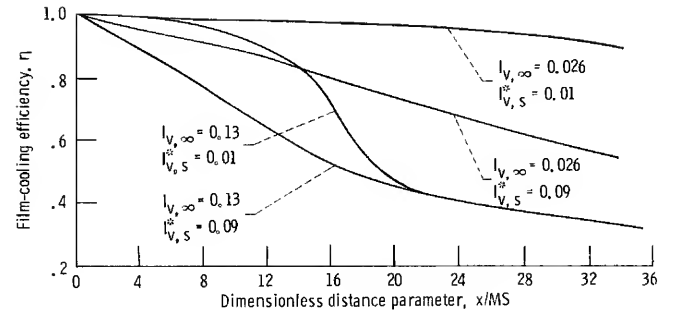


Figure 7.—Effect of coolant turbulence on film-cooling efficiency,  $M = 0.9$ .

Kacker and Whitelaw (ref. 11) reported no effect of the slot turbulence level on the film-cooling efficiency for a 100 percent variation in slot turbulence. The results of reference 11 were for an  $x/S$  of 50 and 100 which could have been in or near the fully developed region where slot turbulence has little effect. The experimental data of Sturgess (ref. 5) does show an appreciable degree of film-cooling efficiency degradation as the coolant turbulence level increases. It can be expected that a slot design which produces as low a coolant turbulent intensity as possible and which minimizes mixing of the two streams should have good film-cooling efficiency in the region of the slot exit. In addition, analytical models which do not make a distinction between the initial and fully developed regions and assume a fully mixed, fully developed region for the entire length of the surface to be protected can be expected to suffer in validity, especially near the point of coolant injection.

The analytical relations developed in this paper are independent of pressure. This is consistent with the experimental findings of Marek (ref. 12) who performed slot film-cooling experiments in a high-pressure combustor. Reference 12 concludes that for the range of pressures investigated (1 to 20 atm), there is no significant change in the film-cooling effectiveness with pressure.

This paper has emphasized the effect of turbulence intensity on jet mixing as it applies to film cooling. The authors of reference 3 indicated that entrainment of the hot free stream by the coolant jet should also depend on the scale of turbulence of the free stream. The work of Oh and Bushwell (ref. 13) indicates that in addition to velocity fluctuations, the length scale of turbulence also plays an important role in determining the turbulent mixing rate of free-shear layers. According to the results of reference 13, an increase in turbulent length scale (or eddy size) should result in an increased jet mixing with a corresponding decrease in film-cooling efficiency.

## Concluding Remarks

Equations have been developed for predicting slot film-cooling efficiency as a function of flow rate, turbulence level, and temperature of the coolant and the hot main stream. The

analytical results make a distinction between an entrance region where there is a potential for efficient film-cooling and the fully developed region where complete mixing between the hot gases and the coolant is assumed. Constants in the developed equations were determined by using the results of a well-designed film-cooling experiment with controlled values of flow, turbulence, and temperature. The final equations based on analysis and experiment were found to predict the experimental data within an average deviation of  $\pm 4$  percent.

The film-cooling prediction equations presented in this paper should be useful in determining the optimum quantity of cooling air required for protecting the wall of a combustor or of any surface requiring slot film cooling.

Lewis Research Center  
National Aeronautics and Space Administration  
Cleveland, Ohio, July 22, 1986

## Appendix A—Analysis of Film-Cooling Efficiency

The assumptions used in the analysis are given in the section Analysis. Figure 1 depicts the situation to be analyzed, a coolant being injected at the wall of a chamber with a rectangular cross section through which flows a high temperature gas of the same composition as the coolant. The control volume of figure 1(b) expresses the differential quantities of mass flow entrained from the free stream and the turbulent diffusion of mass from zone I (mixing zone) to zone II (potential core). A total mass flow-rate balance for zones I and II may be expressed as follows:

$$m_T + \frac{dm_\infty}{dx} dx = m_T + \frac{dm_T}{dx} dx \quad (A1)$$

which may be integrated to

$$m_T = m_s + m_\infty \quad (A2)$$

or in terms of zone I and zone II (fig. 1(b))

$$m_T = m_{T_I} + m_{T_{II}} = m_s + m_\infty \quad (A3)$$

A differential mass flow-rate balance in zone II (fig. 1(b)) results in the following:

$$m_{T_{II}} + \frac{dm_I}{dx} dx = m_{T_{II}} + \frac{dm_{T_{II}}}{dx} dx - \frac{dh}{h} m_{T_{II}} \quad (A4)$$

where  $dm_I/dx$  represents the mass flow rate from zone I to zone II due to turbulent diffusion in zone II. The last term of equation (A4) accounts for the fraction of the mass flow rate in zone II that ends up in zone I as a result of the sloped interface 0-1.

The height  $h$  of the interface 0-1 may be expressed as

$$h = S \left( 1 - \frac{x}{x_1} \right) \quad (A5)$$

Therefore,

$$\frac{dh}{h} = - \frac{dx}{x_1 - x} \quad (A6)$$

with equation (A6), equation (A4) is expressed

$$\frac{dm_{T_{II}}}{dx} dx + \frac{m_{T_{II}}}{(x_1 - x)} dx = \frac{dm_I}{dx} dx \quad (A7)$$

Equation (A7) is solved for the total mass flow rate  $m_{T_{II}}$  of zone II by multiplying by the integrating factor  $1/(x_1 - x)$  and integrating with  $m_{T_{II}} = m_s$  at  $x = 0$ . The result is

$$\frac{m_{T_{II}}}{m_s} = \left( 1 - \frac{x}{x_1} \right) + \frac{(x_1 - x)}{m_s} \int_0^x \left( \frac{dm_I}{dx} \right) \frac{dx}{(x_1 - x)} \quad (A8)$$

Assuming a constant  $dm_I/dx$  and integrating gives

$$m_{T_{II}} = m_s \left( 1 - \frac{x}{x_1} \right) + \left( \frac{x_1}{x} - 1 \right) \ln \left( \frac{1}{1 - \frac{x}{x_1}} \right) m_I \quad (A9)$$

Utilizing figure 1(b), a differential energy balance may be applied to zones I and II in the same manner as the above differential mass flow balance. The zone II differential energy balance is as follows:

$$\frac{d(m_{T_{II}} \bar{T}_{II})}{dx} dx + \left( \frac{m_{T_{II}} \bar{T}_{II}}{x_1 - x} \right) dx = \frac{d(m_I \bar{T}_I)}{dx} dx \quad (A10)$$

integrating equation (A10) as was done for equation (A7) results in

$$m_{T_{II}} \bar{T}_{II} = m_s T_s \left( 1 - \frac{x}{x_1} \right) + (x_1 - x) \int_0^x \frac{d(m_I \bar{T}_I)}{dx} \frac{dx}{(x_1 - x)} \quad (A11)$$

The zone I differential energy balance is as follows:

$$2 \left[ \frac{d(m_{T_I} \bar{T}_I)}{dx} dx \right] - \left( \frac{m_{T_{II}} \bar{T}_{II}}{x_1 - x} \right) dx = \frac{d(m_\infty T_\infty)}{dx} dx \quad (A12)$$

Combining equations (A10) and (A12) and integrating results in

$$m_{T_{II}} \bar{T}_{II} + m_{T_I} \bar{T}_I = m_s T_s + m_\infty T_\infty \quad (A13)$$

Substituting for  $m_{T_{II}} \bar{T}_{II}$  in equation (A12) with equation (A13) gives

$$\begin{aligned} \frac{d(m_{T_1}\bar{T}_1)}{dx} dx + \left(\frac{m_{T_1}\bar{T}_1}{x_1 - x}\right) dx - \frac{d(m_\infty T_\infty)}{dx} dx - \left(\frac{m_\infty T_\infty}{x_1 - x}\right) dx \\ - \left(\frac{m_s T_s}{x_1 - x}\right) dx = - \frac{d(m_1\bar{T}_1)}{dx} dx \end{aligned} \quad (A14)$$

Multiplying equation (14) by the integrating factor  $1/(x_1 - x)$  and integrating produces the following:

$$m_{T_1}\bar{T}_1 = m_s T_s \frac{x}{x_1} + m_\infty T_\infty - (x_1 - x) \int_0^x \frac{d(m_1\bar{T}_1)}{dx} \frac{dx}{(x_1 - x)} \quad (A15)$$

$m_{T_1}$  may be determined by utilizing equations (A3) and (A9) resulting in

$$m_{T_1} = m_s \frac{x}{x_1} + m_\infty - (x_1 - x) \int_0^x \frac{d(m_1)}{dx} \frac{dx}{(x_1 - x)} \quad (A16)$$

Substituting for  $m_{T_1}$  in equation (A15) and solving for  $\bar{T}_1$  gives

$$\begin{aligned} \bar{T}_1 = \frac{T_s}{1 + \frac{m_\infty}{m_s \frac{x}{x_1}}} + \frac{T_\infty}{1 + \frac{m_s \frac{x}{x_1}}{m_\infty}} + \frac{(x_1 - x)}{m_s \frac{x}{x_1} + m_\infty} \\ \times \left[ \bar{T}_1 \int_0^x \frac{dm_1}{dx} \frac{dx}{(x_1 - x)} - \int_0^x \frac{d(m_1\bar{T}_1)}{dx} \frac{dx}{(x_1 - x)} \right] \end{aligned} \quad (A17)$$

A mass flow-rate balance of both fluid streams (fig. 1(a)) at position  $x = 0$  and at any other position results in

$$m_T = m_s + \bar{U}_\infty \rho_\infty y_2 \quad (A18)$$

The entrained mass flow rate  $m_\infty$  by comparison with equation (A3) is

$$m_\infty = \bar{U}_\infty \rho_\infty y_2 \quad (A19)$$

Because the edges 0-1 and 0-2 (fig. 1(a)) were assumed to be linear in  $x$ ,  $y_2$  has the following relationship:

$$y_2 = \frac{x}{x_1} (\phi_1 - 1) S \quad (A20)$$

where  $\phi_1 = b_1/S$ .  
Since

$$m_s = \bar{U}_s \rho_s S \quad (A21)$$

$$M = \bar{U}_s e_s / \bar{U}_\infty \rho_\infty \quad (A22)$$

use of equations (A19) to (A22) results in the following equation for the average temperature in zone I for  $x < x_1$ :

$$\begin{aligned} \bar{T}_1 = \frac{T_s}{1 + \frac{(\phi_1 - 1)}{M}} + \frac{T_\infty}{1 + \frac{M}{\phi_1 - 1}} + \frac{(x_1 - x)}{m_s \frac{x}{x_1} \left(1 + \frac{(\phi_1 - 1)}{M}\right)} \\ \times \left[ \bar{T}_1 \int_0^x \frac{dm_1}{dx} \frac{dx}{(x_1 - x)} - \int_0^x \frac{d(m_1\bar{T}_1)}{dx} \frac{dx}{(x_1 - x)} \right] \end{aligned} \quad (A23)$$

Inspection of equation (A23) indicates that for a given blowing rate  $M$ ,  $T_s$  and  $T_\infty$ , the variation in  $x$  of  $\bar{T}_1$ , will depend only on the last term of equation (A23). This last term can be shown to be quite small so that  $\bar{T}_1$  is determined by the first two terms of equation (A23) which are invariant in  $x$ . Therefore, a useful simplification for zone I for  $x < x_1$  is

$$\bar{T}_1 = \text{constant} \quad (A24)$$

which permits the following identity in the initial region ( $x < x_1$ )

$$\bar{T}_1 = T_{aw_{x=x_1}} \quad (A25)$$

Because of the adiabatic wall assumption, the average temperature of zone II may be expressed

$$\bar{T}_{II} = T_{aw} \quad (A26)$$

Use of equations (A24) to (A26) simplifies equation (A11) and (A15) so that together with equations (A9) and (A16), the energy and mass flow-rate equations for zones I and II (fig. 1) may be expressed for zone I as

$$m_{T_1} T_{aw_{x=x_1}} = m_s f(x) T_s + m_\infty T_\infty - g(x) m_1 T_{aw_{x=x_1}} \quad (A27)$$

$$m_{T_1} = m_s f(x) + m_\infty - g(x) m_1 \quad (A28)$$

and for zone II as

$$m_{T_{II}} T_{aw} = m_s (1 - f(x)) T_s + g(x) m_I T_{aw_{x=x_1}} \quad (A29)$$

$$m_{T_{II}} = m_s (1 - f(x)) + g(x) m_I \quad (A30)$$

where

$$f(x) = \frac{x}{x_1} \quad (A31)$$

$$g(x) = \left( \frac{x_1}{x} - 1 \right) \ln \left( \frac{1}{1 - \frac{x}{x_1}} \right) \quad (A32)$$

Equation (A30) has the expected form for zone II, since as  $x \rightarrow x_1$ ,  $g(x) \rightarrow 0$ , and  $m_{T_{II}} \rightarrow 0$ . Combining equations (A27) and (A29) and substituting for  $m_{T_{II}}$  and  $m_\infty$  (eq. (A3)) results in

$$\frac{m_{T_I}}{m_T} \left( \frac{T_{aw_{x=x_1}} - T_{aw}}{T_s - T_\infty} \right) + \frac{T_{aw} - T_\infty}{T_s - T_\infty} = \frac{m_s}{m_T} \quad (A34)$$

Since the film-cooling efficiency  $\eta$  is defined as

$$\eta = \frac{T_\infty - T_{aw}}{T_\infty - T_s} \quad (A35)$$

Equation (A34) becomes

$$\eta = \frac{m_s}{m_T} + \frac{m_{T_I}}{m_T} \left( \frac{T_{aw_{x=x_1}} - T_{aw}}{T_\infty - T_s} \right) \quad (A36)$$

The last term of equation (A36) is normally neglected in film-cooling calculations. This term accounts for the existence of “potential core” (zone II).

Substituting for  $m_{T_{II}}$  in equation (A29), using equation (A30), and solving for  $m_I$  give

$$m_I = \frac{m_s}{g(x)} \left( 1 - \frac{x}{x_1} \right) \left( \frac{T_{aw} - T_s}{T_{aw_{x=x_1}} - T_{aw}} \right) \quad (A37)$$

Use of equations (A30), (A37), and (A3) results in the following expression for the total mass flow rate of zone I:

$$m_{T_I} = m_T - m_s \left( 1 - \frac{x}{x_1} \right) (1 + \theta) \quad (A38)$$

$$\theta = \frac{T_{aw} - T_s}{T_{aw_{x=x_1}} - T_{aw}} \quad (A39)$$

Substituting equations (A18) and (A20) into equation (A38) results in

$$\frac{m_{T_I}}{m_s} = \frac{x}{x_1} \left[ \frac{\phi_1 - 1}{M} + 1 \right] - \left( 1 - \frac{x}{x_1} \right) \theta \quad (A40)$$

Since  $y_2 = b - S$  (fig. 1(a)) equation (A18) may be expressed

$$\frac{m_s}{m_T} = \frac{1}{1 + \left( \frac{x}{MS} \right) \left( \frac{(\phi - 1)S}{x} \right)} \quad (A41)$$

where  $\phi = b/S$ .

Equation (A36) may be expressed in terms of the efficiency  $\eta'$  that would be predicted by neglecting the “potential core” (zone II) (i.e., a fully mixed zone I and II)

$$\eta' = \frac{m_s}{m_T} = \frac{\eta}{\left[ 1 + \frac{m_{T_I}}{m_s} \left( \frac{T_{aw_{x=x_1}} - T_{aw}}{T_\infty - T_s} \right) \right]} \quad (A42)$$

where  $\eta$  = the experimental film-cooling efficiency.

Using equations (A40) and (A41) results in equation (A42) being expressed as follows:

$$\eta' = \frac{\eta}{1 + \beta_{\text{exp}}} = \frac{1}{1 + \left( \frac{x}{MS} \right) \left( \frac{(\phi - 1)S}{x} \right)} \quad (A43)$$

where

$$\beta_{\text{exp}} = \left[ \frac{x}{x_1} \left( \frac{\phi_1 - 1}{M} + 1.0 \right) - \left( 1 - \frac{x}{x_1} \right) \theta \right] \psi \quad (A44)$$

$$\theta = \frac{T_{aw} - T_s}{T_{aw_{x=x_1}} - T_{aw}}$$

$$\psi = \frac{T_{aw_{x=x_1}} - T_{aw}}{T_\infty - T_s}$$

For determining a general value of  $\beta$  for equation (A42) that will account for turbulent diffusion in zone II, equation (A16) is combined with equations (A19) and (A20) to obtain

$$\beta = \left[ \frac{x}{x_1} \left( \frac{\phi_1 - 1}{M} + 1.0 \right) - \frac{x_1 - x}{m_s} \int_0^x \left( \frac{dm_1}{dx} \right) \frac{dx}{(x_1 - x)} \right] \psi \quad (\text{A45})$$

The turbulent diffusion of mass from zone I to zone II ( $dm_1/dx$ ) may be expressed in terms of the jet lateral fluctuating velocity  $\bar{v}'_{s,o}$  and the density  $\rho_1$  of zone I as follows:

$$\frac{dm_1}{dx} \approx \bar{v}'_{s,o} \rho_1 \quad (\text{A46})$$

A more exact form of the derivative may be obtained from an approximation which utilizes equation (A37) and assumes a linear variation in  $x$  of the wall temperature  $T_{aw}$

$$\left( \frac{dm_1}{dx} \right)_{\text{exp}} \approx \frac{\bar{U}_s \rho_s S}{x_1} \quad (\text{A47})$$

Therefore, the mass flow rate from zone I to II may be expressed as

$$\frac{dm_1}{dx} = \frac{C_o \bar{v}'_{s,o} \rho_1 S}{x_1} \quad (\text{A48})$$

Substituting equation (A48) in equation (A45) results in the following:

$$\beta = \left[ \frac{x}{x_1} \left( \frac{\phi_1 - 1}{M} + 1.0 \right) - \left( \frac{x_1 - x}{x_1} \right) C_o I_{v,s}^* \frac{T_s}{T_{aw,x=x_1}} \ln \left( \frac{1}{1 - \frac{x}{x_1}} \right) \right] \psi \quad (\text{A49})$$

where

$$I_{v,s}^* = \frac{\bar{v}'_{s,o}}{\bar{U}_s} \quad (\text{A50})$$

The value of the constant  $C_o$  may be determined by utilizing experimental data.

Inspection of equations (A44) and (A49) indicates that the value of  $\beta$  became zero at the end of the initial region ( $x = x_1$ ). The equation for the fully developed region ( $x \geq x_1$ ) is therefore

$$\eta = \frac{1}{1 + \left( \frac{x}{MS} \right) \left( \frac{(\phi - 1)S}{x} \right)} \quad (\text{A51})$$

or in terms of a turbulent mixing coefficient  $C_M$  (refs. 2 and 3)

$$\eta = \frac{1}{1 + \left( \frac{x}{MS} \right) C_M} \quad (\text{A52})$$

where the turbulent mixing coefficient in the present analysis is a function of the jet boundary layer growth rate

$$C_M = \frac{(\phi - 1)S}{x} \quad (\text{A53})$$

The efficiency equations (A43) and (A51) for the initial and developed regions maybe expressed in a general equation

$$\eta = \frac{1}{1 + \left( \frac{x}{MS} \right) C'_M} \quad (\text{A54})$$

where

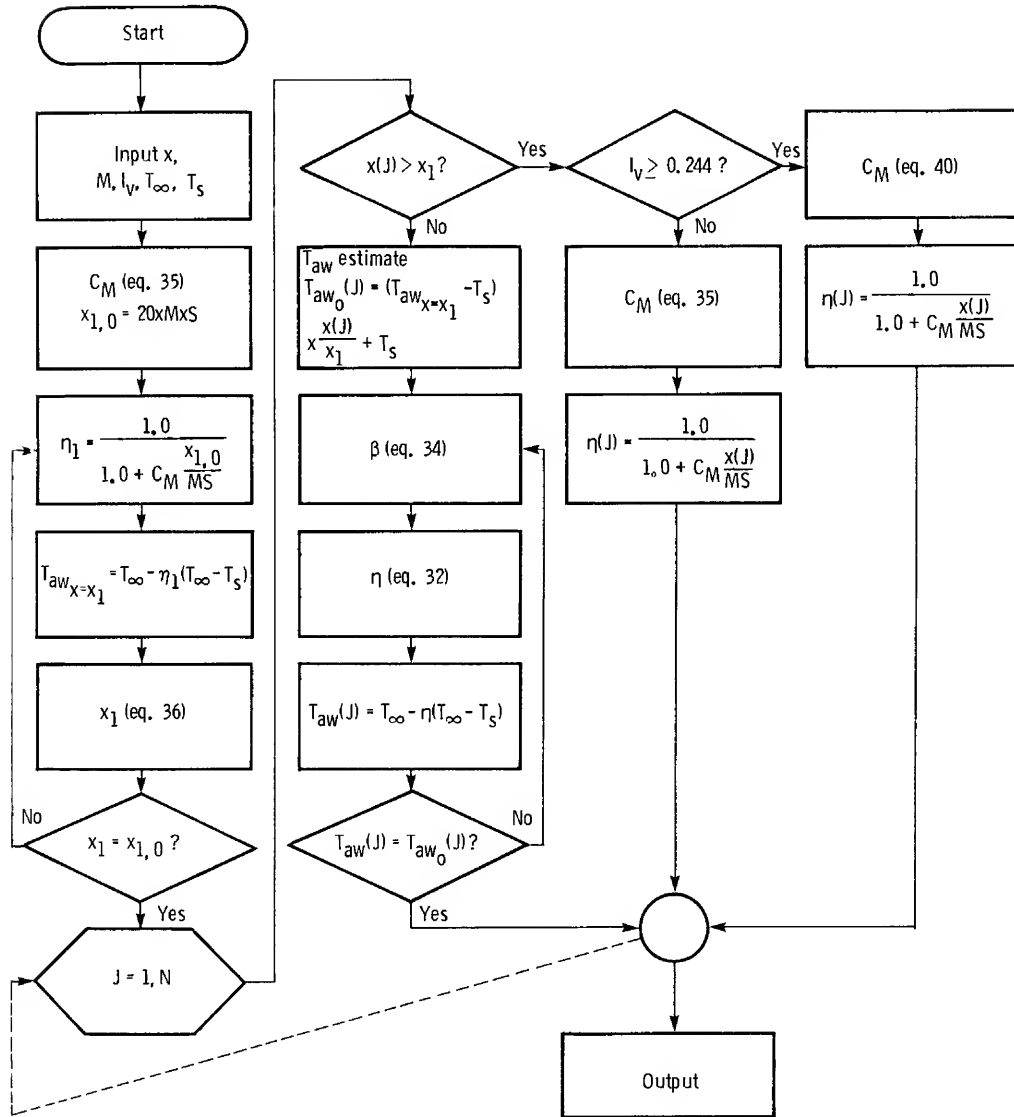
$$C'_M = \frac{C_M - \frac{\beta}{\left( \frac{x}{MS} \right)}}{1 + \beta} \quad (\text{A55})$$

with the following conditions:

$$x \geq x_1 \quad \begin{cases} \beta = 0 \\ C'_M = C_M \end{cases}$$

## Appendix B

### Film-Cooling Efficiency Computational Flow Chart



## References

1. Carlson, L.W.; and Talmor, E.: Gaseous Film Cooling at Various Degrees of Hot-Gas Acceleration and Turbulence Levels. *Int. J. Heat Mass Trans.*, vol. 11, no. 11, Nov. 1968, pp. 1695-1713.
2. Juhasz, A.J.; and Marek, C.J.: Combustor Liner Film Cooling in the Presence of High Free Stream Turbulence. NASA TN D-6360, 1971.
3. Marek, C.J.; and Tacina, R.R.: Effect of Free Stream Turbulence on Film Cooling. NASA TN D-7958, 1975.
4. Sturgess, G.J.; and Lenertz, J.E.: Account of Mainstream Turbulence for Predicting Film Cooling Effectiveness of Gas Turbine Combustors. ASME Paper 77-HT-10, Aug. 1977.
5. Sturgess, G.J.: Account of Film Turbulence for Predicting Film Cooling Effectiveness in Gas Turbine Combustors. *J. Eng. Power*, vol. 102, no. 3, July 1980, pp. 524-534.
6. Sturgess, G.J.: Correlation of Data and Prediction of Effectiveness From Film Cooling Injection Geometries of a Practical Nature. *Combustion and Heat Transfer in Gas Turbine Systems*, vol. 11, E.R. Norster, ed., Pergamon Press, 1971, pp. 229-250.
7. Abramovich, G.N.: *The Theory of Turbulent Jets*. MIT Press, 1963.
8. Sturgess, G.J.; and Pfeifer, G.D.: Design of Combustor Cooling Slots for High Film Effectiveness, Part II-Film Initial Region. *J. Eng. Gas Turbines Power*, vol. 108, no. 2, Apr. 1986, pp. 361-369.
9. Cohen, L.S.: A Kinematic Eddy Viscosity Model Including the Influence of Density Variations and Preturbulence. *Free Turbulent Shear Flows*, vol. 1, NASA SP-321, 1972, pp. 139-183.
10. Ko, S.-Y.; and Liu, D.-Y.: Experimental Investigation on Effectiveness, Heat Transfer Coefficient, and Turbulence of Film Cooling. *AIAA J.*, vol. 18, no. 8, Aug. 1980, pp. 907-913.
11. Kacker, S.C.; and Whitelaw, J.H.: The Effect of Slot Height and Slot Turbulence Intensity on the Effectiveness of the Uniform Density, Two-Dimensional Wall Jet. *J. Heat Trans.*, vol. 90, no. 4, Nov. 1968, pp. 469-475.
12. Marek, C.J.: Effect of Pressure on Tangential-Injection Film Cooling in a Combustor Exhaust Stream. NASA TM X-2809, 1973.
13. OH, Y.H.; and Bushnell, D.M.: Influence of External Disturbances and Compressibility on Free Turbulent Mixing. *Aerodynamic Analysis Requiring Advanced Computers, Part I*, NASA SP-347, 1975, pp. 341-376.

1. Report No. NASA TP-2655	2. Government Accession No.	3. Recipient's Catalog No.	
4. Title and Subtitle Jet Model for Slot Film Cooling With Effect of Free-Stream and Coolant Turbulence		5. Report Date October 1986	
		6. Performing Organization Code 505-62-21	
7. Author(s) Frederick F. Simon		8. Performing Organization Report No. E-2961	
		10. Work Unit No.	
9. Performing Organization Name and Address National Aeronautics and Space Administration Lewis Research Center Cleveland, Ohio 44135		11. Contract or Grant No.	
		13. Type of Report and Period Covered Technical Paper	
12. Sponsoring Agency Name and Address National Aeronautics and Space Administration Washington, D.C. 20546		14. Sponsoring Agency Code	
15. Supplementary Notes			
16. Abstract  An analysis was performed utilizing the model of a wall jet for obtaining equations that will predict slot film-cooling efficiency under conditions of variable turbulence intensity, flow, and temperature. The analysis, in addition to assessing the effects of the above variables, makes a distinction between an initial region and a fully developed region. Such a distinction is important in determining the role that the turbulence intensity of the coolant plays in effecting film-cooling effectiveness in the area of the slot exit. The results of the analysis were used in the correlation of the results of a well-designed film-cooling experiment. The result of the analysis and experiment was equations that predicted film-cooling efficiency within $\pm 4$ percent average deviation for lateral free-stream turbulence intensities up to 24 percent and blowing rates up to 1.9. These equations should be useful in determining the optimum quantity of cooling air required for protecting the wall of a combustor.			
17. Key Words (Suggested by Author(s)) Film cooling, Effect of turbulence, Effect of flow rate, Initial region, Fully developed region		18. Distribution Statement Unclassified—unlimited STAR Category 34	
19. Security Classif. (of this report) Unclassified	20. Security Classif. (of this page) Unclassified	21. No of pages 20	22. Price* A02

\*For sale by the National Technical Information Service, Springfield, Virginia 22161

NASA-Langley, 1986